Volatilisation of Trace Elements During Evaporation to Dryness of HF-Dissolved Silicates (BHVO -2, AGV -1, BIR -1, UB-N): Open- Versus Closed-System Conditions

Ivan Vlastélic, Jean-luc Piro

Vol. 46 — N° 3 09 22 p. 519 – 534

GEOSTANDARDS and GEOANALYTICAL RESEARCH

Volatilisation of Trace Elements During Evaporation to Dryness of HF-Dissolved Silicates (BHVO-2, AGV-1, BIR-1, UB-N): Open- *Versus* Closed-System Conditions

Ivan **Vlastelic*** and Jean-Luc **Piro**

Laboratoire Magmas et Volcans, CNRS, IRD, OPGC, Université Clermont Auvergne, Clermont-Ferrand F-63000, France
* Corresponding author. e-mail: ivan.vlastelic@uca.fr

This work characterises the volatilisation of trace elements during evaporation to dryness of HF-dissolved silicate rock reference materials (BHVO-2, AGV-1, BIR-1, UB-N). In open-system conditions, sublimation at 80 °C remained small (≤ 3%) for most elements with the exception of boron. Conversely, during closed-system evaporation in a PTFE elbow, volatilisation loss could exceed 3% for Te, Au, Se, Ru, B, Re, As, V and Ge; 100 µg g^{-1} for Pt, Cd, Ag, Mo and Ti; and 10 µg g^{-1} for many refractory elements including Nb, Hf, U and Yb. Higher volatilisation loss in the closed-system results from the higher vapour pressure of HF that allows for the formation of highly fluorinated species with lower sublimation temperature, or unstable species such as rare earth tetrafluorides for which sublimation competes with thermal decomposition. Increasing the temperature from 50 to 100 °C promotes the formation and sublimation of highly fluorinated species (VF_5, GeF_4, SeF_6). Conversely, some refractory elements (Hf, Zr, Yb, U, Cu, Zn, Rb, Ba and Sr) seem to preferentially sublimate at 50 °C possibly through the formation of hydrated fluorides. Our results indicate that closed-system evaporation must be used with caution for quantitative analyses.

Keywords: silicate dissolution, hydrofluoric acid, trace elements, evaporation, sublimation, closed-system.

Received 02 Sep 21 – Accepted 20 Mar 22

Dissolution of silicate rocks for the purpose of bulk chemical or isotope determination is routinely achieved using a mixture of hydrofluoric acid and a strong acid with a higher boiling temperature, such perchloric or nitric acid. This dissolution method is both convenient and efficient but leads to the formation of poorly soluble and volatile fluorides, which prevents the total recovery of several elements (Yokoyama *et al.* 1999, Hu and Qi 2014). In particular, metalloids (Si, B, As, Ge, Sb, Te), non-metals (P, Se) and transition metals (Mo, V, W, Re, Ru, Ir, Os) with high valence states (≥ III) tend to form volatile fluorides (Table 1) that are potentially lost during the evaporation stage. On the one hand, quantitative loss of Si as volatile SiF_4 (boiling point of -86 °C) limits the formation of fluoride salts, which facilitates further treatment of the samples. On the other hand, fluoride volatilisation becomes a major issue for the determination of moderately volatile elements, such as B, As, Sb and Ge but also refractory transition metals such as Re, Os, Ir, Pt and possibly Ti, Nb and Ta (Sulcek *et al.* 1977, Bajo 1978, Bock 1979, Ishikawa and Nakamura 1990, Chao and Sanzolone 1992). This issue is critical because thermodynamic data for pure compounds are only indicative and do not allow the timing and extent of element volatilisation from natural samples to be predicted. The reason for this is that atomic forces between ions and molecules that govern the chemical potentials in HF-dissolved silicates are not known. In addition, due to the extreme electronegativity of F, metals bound to F ions lose part of their metallic properties in the solid precipitate and tend to sublimate. This effect increases with coordination number and is critical for transition metal penta- and hexafluorides that form nearly spherical-shaped molecules with weak intermolecular forces (Molski and Seppelt 2009). To prevent fluoride precipitation and trace element volatilisation, evaporations of HF-digested silicates are generally conducted at low temperature (below 85 °C) and/or to incipient dryness (e.g., Luais 2012, Yierpan *et al.* 2018). Alternatively, Menard *et al.* (2013) proposed a method avoiding sample evaporation for boron

doi: 10.1111/ggr.12428

Table 1.
Boiling or sublimation point (°C) of selected fluorides

Valence state	VI		V		IV		III		III/II		I	
B							BF_3	-100				
Si					SiF_4	-86	Si_2F_6	-19	Si_3F_8	42		
P			PF_5	-75			PF_3	-102				
S	SF_6	-64	S_2F_{10}	30	SF_4	-40						
Ti					TiF_4	284	TiF_3	950				
V			VF_5	48	VF_4	325	VF_3	1395				
Cr			CrF_5	117	CrF_4	400	CrF_3	1200				
Ge					GeF_4	-37			GeF_2	130		
As			AsF_5	-52.8			AsF_3	57				
Se	SeF_6	-47			SeF_4	102						
Zr					ZrF_4	912						
Nb			NbF_5	236								
Mo	MoF_6	34	MoF_5	215								
Ru	RuF_6	200*	RuF_5	227			RuF_3	650*				
Rh	RhF_6	70					RhF_3	600				
Ag									AgF_2	700*	AgF	1159
In							InF_3	> 1200				
Sn					SnF_4	705			SnF_2	850		
Sb			SbF_5	141			SbF_3	376				
Te	TeF_6	-39	Te_2F_{10}	59	TeF_4	195*						
Ce					CeF_4	600*	CeF_3	2180				
Pr					PrF_4	90*						
Tb					TbF_4	300*	TbF_3	2280				
Hf					HfF_4	970						
Ta			TaF_5	229								
W	WF_6	17	WF_5	20*	WF_4	800						
Re	ReF_6	34	ReF_5	221	ReF_4	300						
Ir	IrF_6	54					IrF_3	250*				
Pt	PtF_6	69			PtF_4	600 m.p.						
Au			AuF_5	0*			AuF_3	300				
Tl							TlF_3	550*			TlF	826
Bi			BiF_5	230			BiF_3	900				
U	UF_6	56			UF_4	1417						

Data source: Rumble (2021) – Physical constants of inorganic compounds.
* Decomposition; m.p. melting point.

determination. While the issue of the volatility of fluorides is well known, there are few reviews on this topic, and these are mostly based on thermodynamic data of pure compounds (e.g., Makishima 2016).

This study aims to better understand the fundamental processes that control the timing and extent of volatilisation of trace elements during the evaporation to dryness of HF-dissolved silicates. Such information is needed to adjust evaporation procedures and quantify more precisely the abundance of elements forming volatile fluorides in silicate rocks. It is also useful in radiochemistry where gaseous emissions of radioactive species, as small they are, must be monitored (Pérot *et al.* 2018). We present results of evaporation experiments conducted at low temperatures (50–100 °C) suitable for the determination of volatile trace elements (e.g., Luais 2012, Yierpan *et al.* 2018). These experiments constrain in particular the sublimation loss of elements during drying. For the majority of elements, with the exception of Si and B, the sublimation losses are small and cannot be precisely quantified by mass balance from the residue. Here, we use transpiration-cell mass spectrometry to monitor the flux of gaseous elements escaping from an HF-dissolved basalt during evaporation to dryness. We also evaluate trace element volatilisation when evaporation is conducted in a closed system (PTFE elbow), which represents a promising way to reduce procedural blanks and acid gas emissions to the environment. Closed system evaporation is still not widely used in multi-element determination in geological samples, and the behaviour of elements in such conditions is not known. Quite unexpectedly, our results show that the volatilisation loss of trace elements is higher when evaporation is conducted in a PTFE elbow than during conventional open-system evaporation.

Experimental

This work first focused on the Hawaiian basalt BHVO-2 provided by the USGS. This typical ocean island basalt with 49.9 g/100 g SiO_2, 13.5 g/100 g Al_2O_3, 12.3 g/100 g Fe_2O_3, 11.4 g/100 g CaO, 7.23 g/100 g MgO, 2.74 g/100 g total alkali and 0.27 g/100 g P_2O_5 is one of the best characterised and most employed geological reference materials (Jochum *et al.* 2016). To evaluate how rock composition affects trace element volatilisation we also analysed a basalt with higher MgO content (USGS BIR-1 with 9.7 g/100 g MgO), an andesite (USGS AGV-1 with 1.51 g/100 g MgO) and a serpentinite (UB-N from the CRPG with 35.2 g/100 g MgO). All experiments are summarised in Table 2.

Open system sublimation, BHVO-2 basalt (experiment 1)

A first experiment was designed to quantify element loss during open-system sublimation, which represents the most common situation. One gram of BHVO-2 powder (batch 759) was precisely weighed into a 60 ml screw-top PFA jar (part 100-0060-01, Savillex, Eden Prairie, USA). Following a

Table 2.
Summary of experiments and analyses

	Experiment 1 (open system)	Experiment 2a (closed system)		Experiment 2b (closed system)
Test portion (mass)	BHVO-2 (1 g)	BHVO-2 (300 mg × 6)		BIR-1a, AGV-1, UB-N (300 mg each)
Vessel type	60 ml Savillex part 100-0060-01	30 ml Savillex part 200-030-20		30 ml Savillex part 200-030-20
Dissolution	10 ml of 7 mol l^{-1} HNO_3 20 ml of 29 mol l^{-1} HF 80 °C for 48 h	3 ml 14 mol l^{-1} HNO_3 6 ml of 29 mol l^{-1} HF 80 °C for 48 h		3 ml 14 mol l^{-1} HNO_3 6 ml of 29 mol l^{-1} HF 80 °C for 48 h
		Batch 1–3	**Batch 4–6**	
Evaporation	80 °C Open system, without vapour recovery Hot plate in a laminar flow hood Stopped before drying	50–80–100 °C Closed system, with vapour recovery Analab evapoclean EV-6.25 ml Stopped before drying Collection of vapour condensates (evaporation only)	50–80–100 °C Closed system, with vapour recovery Analab evapoclean EV-6.25 ml Stopped 6–8 h after drying Collection of vapour condensates (evaporation plus sublimation)	100 °C Closed system, with vapour recovery Analab evapoclean EV-6.25 ml Stopped 6–8 h after drying Collection of vapour condensates (evaporation plus sublimation)
Drying/Sublimation	80 °C	50–80–100 °C	x	
	Open system Sublimation vapours vented into ICP-MS	Open system without vapour recovery (Drying of the residue on a hot plate)		
Analysis of vapours	Yes, online	Yes (condensates)		Yes (condensates)
		Evaporation of the condensates to near dryness at 30 °C		Evaporation of the condensates to near dryness at 30 °C
		Dilution of the liquid residues with 3 ml of 0.5 mol l^{-1} HNO_3–0.05 mol l^{-1} HF for ICP-MS analysis		Dilution of the liquid residues with 3 ml of 0.5 mol l^{-1} HNO_3–0.05 mol l^{-1} HF for ICP-MS analysis
Analysis of the dry residue	No	Yes		No
		Addition of 2 ml of 14 mol l^{-1} HNO_3		
		Evaporation (50–80–100 °C) in closed system with vapour recovery		
		Dilution and ICP-MS analysis of vapour condensates		
		Full dissolution (7 mol l^{-1} HNO_3) and dilution of the solid residues for ICP-MS analysis		

rather conventional procedure (e.g., Sulcek *et al.* 1977), we added 10 ml of 7 mol l^{-1} HNO_3 and 20 ml of 29 mol l^{-1} HF so that the HF/SiO_2 molar ratio (~ 69) was much higher than the stoichiometric ratio of 4 ($SiO_{2(s)}$ + $4HF_{(l)}$ → $SiF_{4(g)}$ + $2H_2O_{(l)}$). We used 7 mol l^{-1} instead of 14 mol l^{-1} HNO_3 to protect the ICP-MS during the evaporation experiment. Both acids, originally of analytical grade, were purified with a DST-1000 acid purification system (Savillex, Eden Prairie, USA) before use. The closed jar was placed on a hot plate at 80 °C for 48 h. Evaporation was conducted at 80 °C on a hot plate in a laminar flow hood and stopped before drying when the remaining solution (~ 1 ml) started to become gelatinous. The jar containing the BHVO-2 gelatinous residue was closed with a transfer closure and was moved onto a hot plate plate adjacent to a 7500 Series quadrupole ICP-MS (Agilent Technologies, Santa Clara, USA) for the evaporation experiment (Figure 1a). The jar was placed on a hot plate with a rack that allowed for homogeneous heating. A mixture of high purity inert gases (0.85 l min^{-1} Ar, 0.85 l min^{-1} He and 2.5 ml min^{-1} N_2) was heated at the same temperature as the sample using a warmed serpentine system prior to being introduced into the vial through its inlet port. The inert gases and the trace gases that emanated from the sample were vented through the vial outlet port and introduced into the ICP-MS using a quartz torch (Figure 1a). With such flow rates, the residence time of gases in the jar was *ca.* 2.1 s. To improve ICP-MS sensitivity, we used high-sensitivity lenses (Cs type) and two primary pumps increasing the vacuum of the interface. For the same reason, we did not use the *octopole reaction system* but acquired data in no-gas mode. Before the evaporation experiment, the ICP-MS was tuned under dry plasma conditions by coupling the spectrometer with a laser ablation system. All system parameters were tuned to obtain the best sensitivity, to reduce the formation of oxide and double-charged ions and to perform the detector

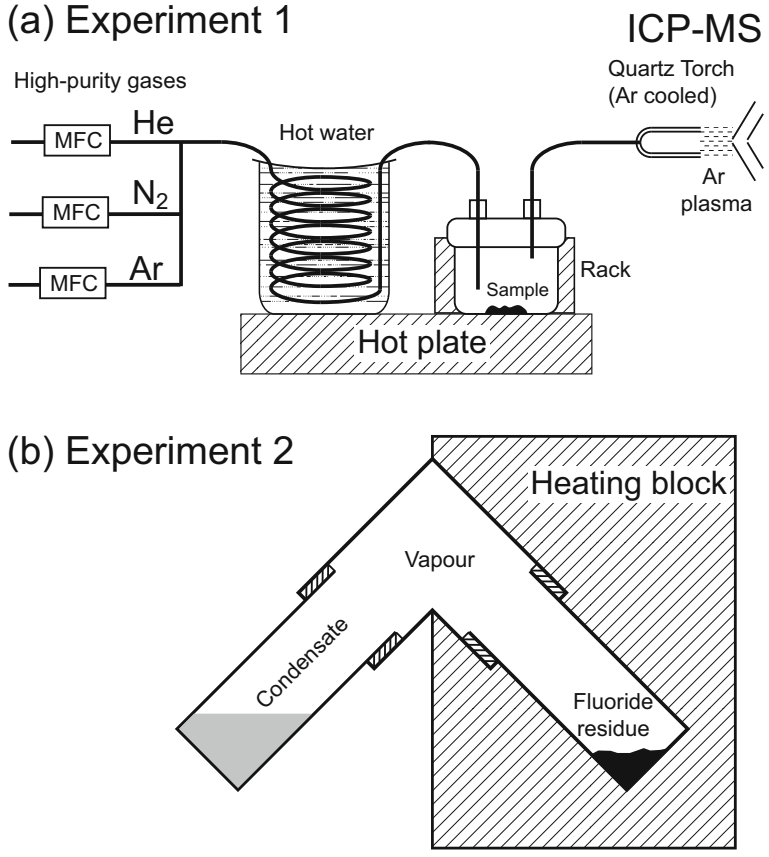

Figure 1. Experimental setup. (a) Drawing showing the experimental setup for direct analysis of the vapour during open-system evaporation (Experiment 1). Evaporation to dryness of HF-dissolved BHVO-2 was conducted in a jar with transfer closure (Savillex, Eden Prairie, USA). The vapours emanating from the sample during drying were swept by a mixture of Ar-He-N_2 inert gases and evacuated into a 7500 Series quadrupole ICP-MS (Agilent Technologies, Santa Clara, USA) for online analysis. MFC – mass flow controller. (b) Drawing of the EV-6.25 ml Evapoclean device (Analab, Hoenheim, France) used to perform closed-system evaporations (Experiment 2).

calibration. Data were acquired in time-resolved analysis mode. Fifty-seven elements were measured using the mass numbers recommended for no-gas mode. The scanning period was 4.47 s, which is about two times the residence time of gases in the sample jar. All operating conditions are summarised in Table 3. The plate was kept at room temperature during the first 10 min of data acquisition. Following this the plate temperature was set at 60 °C for 1 h (600 s $< t <$ 4200 s) to evaporate gently the remaining HF-HNO_3 acid mixture. The temperature was then raised to 70 °C and to 80 °C 30 min later (t = 6000 s). The disappearance of the O_2 and NO_x signals and the simultaneous boron sublimation peak indicated that the residue dried up at 6420 ± 20 s. The temperature was then raised to 90 °C at 8940 s and to 100 °C at 10140 s.

Closed system sublimation (experiment 2)

A second experiment was designed to investigate element sublimation during closed-system evaporation and the role of temperature. Closed-system evaporation is a promising solution to reduce sample contamination and to avoid acid gas emissions to the atmosphere or environment. In this case, total vapour recovery also allowed us to precisely quantify the amount of element volatilised. In experiment 2a, six aliquots (~ 300 mg each) of BHVO-2 powder, batch 759, were weighed into 30 ml screw-top PFA vials (part 200-030-20, Savillex, Eden Prairie, USA). Each aliquot was dissolved in a mixture of 3 ml of 14 mol l^{-1} HNO_3 and 6 ml of 29 mol l^{-1} HF at 80 °C for 48 h. After cooling, the samples were evaporated in a closed system EV-6.25 ml Evapoclean device (Analab, Hoenheim, France) allowing for the recovery of the HF-HNO_3 vapours (Figure 1b). Evaporations were conducted at 50 °C (two samples), 80 °C (two samples) and 100 °C (two samples). In all cases, the temperature was constant during heating. For each sample pair evaporated at the same temperature, evaporation was stopped just before drying for one sample (gelatinous consistency) and 6–8 h after drying for the other sample to allow for potential sublimation processes. The heating time required for near-complete evaporation was 8 h at 100 °C, 16 h at 80 °C and 96 h at 50 °C, for a room temperature of 22 °C (condensate temperature). The experiments performed at 50 and 100 °C with complete evaporation were duplicated. All eight HF-HNO_3 vapour condensates (9 ml) were evaporated slowly for 2 months at 30 °C until near dryness in the Evapoclean device to preserve as much as possible volatile species in the liquid residue. The residual drops were then diluted in 3 ml of 0.5 mol l^{-1} HNO_3-0.05 mol l^{-1} HF for ICP-MS analysis (which corresponded to a factor of 9/3 = 3 concentration of the condensates). After drying the three gelatinous residues on a hot plate, all dry residues were taken with 2 ml of 14 mol l^{-1} HNO_3 and evaporated to dryness at the same temperatures as during the first step. The HNO_3 vapours collected at this stage were directly diluted with 30 ml of 0.05 mol l^{-1} HF for ICP-MS analysis. The dry residues were then totally dissolved in 110–115 g of 7 mol l^{-1} HNO_3. The clear solutions were further diluted with 0.05 mol l^{-1} HF to reach a dilution factor ($m_{solution}$/m_{BHVO} ~ 5200) and acid concentration (0.5 mol l^{-1} HNO_3-0.05 mol l^{-1} HF) suitable for trace element determination by ICP-MS. Experiment 2a was repeated for other rock types (AGV-1, BIR-1 and UB-N) at 100 °C (experiment 2b).

Table 3.
ICP-MS operating conditions (Experiment 1)

Parameter	Value
ICP-MS instrument	Agilent 7500
Lenses	Cs
Sampling and skimmer cones	Ni
RF power forward	1350 W
RF power reflected	1 W
Octopole RF	156 V
Q pole parameters (AMU gain)	127
Torch sample depth	4.9 mm
Ar carrier gas	0.85 l min^{-1}
He gas	0.85 l min^{-1}
N_2 gas	2.5 ml min^{-1}
Torch injector	Quartz
Sample cell	Savillex 60 ml jar with two-tube ports
High-sensitivity mode	Two primary pumps on interface
Extract 1	3.6 V
Extract 2	-121.5 V
Omega bias Cs	-78 V
Omega lens Cs	11.6 V
Data acquisition parameters	
Acquisition mode	Time-resolved analysis
Detection mode	Auto
Integration time/mass	0.06 s
Points per mass/sampling period	1
Sampling period	4.5 s
Desolvating nebuliser system*	ESI Apex Omega
Nebuliser	PFA ST 100 µl min^{-1}
Ar gas	3 l min^{-1}
N_2 gas	3 ml min^{-1}
Spray chamber temperature	140 °C
Peltier cooler temperature	3 °C
Desolvating system temperature	155 °C

* Signal calibration in dry plasma mode.

Data acquisition

Raw data acquired during the transpiration experiment were corrected for the background signal measured at the end of the evaporation phase, just prior to the sublimation peak (4200 s $< t <$ 6000 s). At this point, called eutonic with reference to evaporation of saline waters (Babel and Schreiber 2014), neither evaporation nor sublimation

occurs, and the measured signal corresponds to the gas blank. The ICP-MS response in counts per nanogram of element (CPng = counts per second/mass of element entering the ICP-MS per second) was estimated in dry plasma mode using an Apex Omega Desolvating Nebuliser System (DNS) with a PFA spray chamber (Elemental Scientific, Omaha, USA). A solution containing 500 ng l^{-1} of each of the fifty-seven studied elements, prepared by dilution of a 10 mg l^{-1} certified standard solution (Inorganic venture, Christiansburg, USA), was introduced using a 100 µl min^{-1} PFA ST nebuliser with a measured efficiency of 14.4%. The DNS settings are reported in Table 3 and the corresponding ICP-MS response is reported in Appendix S1 (Table 4a). To correct for the blank, we measured the 0.5 mol l^{-1} HNO_3 acid used to dilute the standard solution. With instrument and acquisition settings as those used for the experiment (Table 3), the response ranged between 2×10^6 counts per ng for ^{77}Se to 1639×10^6 counts per ng for ^{159}Tb (Appendix S1, Table 4a). These values were used to convert the measured signals (in count per second) into element mass fluxes (in nanogram of element per second). The mass of the element sublimated was estimated by integrating the signal over the sublimation peak. The high boron signal during the sublimation peak was monitored with $^{11}B^{16}O$, assuming the contribution from ^{27}Al was negligible (the sublimation temperature of AlF_3 being 1272 °C). The ^{11}B signal was calculated using the $^{11}B^{16}O/^{11}B$ ratio of 0.0275 that was measured during the onset of the sublimation peak, assuming this value remained constant during B sublimation.

The solutions of vapour condensates and the dissolved residues from the second experiment were analysed in plasma robust mode (1550 W), using the collision cell (He mode) to reduce interferences on masses ranging from 51 (V) to 77 (Se). The signal was calibrated 'externally' (every four samples) with a synthetic standard solution (Inorganic Venture, Christiansburg, USA) containing 2 µg l^{-1} of Ru, Rh, Pd, Te, Re, Ir, Pt, Au and 10 µg l^{-1} of other elements in the same acid media as samples (0.5 mol l^{-1} HNO_3–0.05 mol l^{-1} HF). We also ran highly diluted standard solutions (1–100 ng l^{-1}) to check the linear response of the ICP-MS within the low concentration range of the vapour condensates. The acid media were also measured every four samples to correct for background signal. Repeated analysis of the acid media yielded 3*s* detection limits after instrumental drift correction < 100 pg g^{-1} for Ti, < 60 pg g^{-1} for Se, B and Zr, < 40 pg g^{-1} for Cu, V and Te, < 10 pg g^{-1} for Cr, Mn, Ni, Zn, Sr and Ba, < 5 pg g^{-1} for Li, Co, Ga, Ge, As, Rb, Cs and Au, and between 0.3 and 2 pg g^{-1} for other elements reported. The relative standard deviation (RSD) of individual determinations (ten repeated measurements) was $< 20\%$ for B, Li, As, Sn, V, Cu, W, Ba, La, Ce, Y, Nb, Ta, Ti, Zr, Hf and Pb, $< 40\%$ for Bi, Sb, Mo, Ge, Se, Te, Pt, Au, Rh, Ru, Ag, Re, Zn, Tl, Mn, U, Th, Pr and Cs, $< 60\%$ for Be, Ni, Co, Cd, In, Ir, Nd, Sm, Eu, Gd, Tb, Dy and Er and $< 80\%$ for Tm, Yb, Lu, Cr, Ga, Rb and Sr. These relatively large RSDs reflect the often very low abundance of elements in the vapour condensates. Full procedural blank performed following 80 °C digestion, 100 °C evaporation and 30 °C concentration of the condensate was above the ICP-MS detection limit for Ti (18 ng), W (5 ng), Zr (0.7 ng), Cr (0.3 ng), As (82 pg), Li (70 pg), Nb, Ta and Mo (20–30 pg), Ce, Hf and Th (10–18 pg), Y, La, Nd and Sm (4–8 pg). Note that the strong enrichment in HF vapours of platinum-group elements (PGE) and gold (relative to elements interfering during ICP-MS measurement) allows their abundances to be measured without preliminary separation. For dry residues, samples from the 80 and 100 °C experiments were calibrated against the 50 °C residue. Mass fractions of B, Au, Te and PGE were not measured in the residues because of small signals, matrix interferences and memory effects.

Results

Online monitoring of vapour composition (BHVO-2 experiment 1)

Figure 2 reports representative time-resolved signals acquired during the first experiment, where evaporation was conducted in an open system, and vapours were evacuated into the ICP-MS. Silicon, monitored with $^{28}Si^{19}F_3^+$, showed a series of evaporation and sublimation peaks that coincide with the heating steps (60, 80, 90 °C). These peaks possibly correspond to the successive volatilisation of Si-F compounds with increasing boiling temperatures, such as Si_3F_8 (42 °C b.p.) and Si_4F_{10} (85 °C b.p.). Silicon trifluorides $^{28,29,30}Si^{19}F_3^+$ generated major signals at $m/z = 85$–87 which precluded the monitoring of Rb and Sr isotopes, while

Figure 2. Examples of time-resolved signals measured during open-system drying of HF-dissolved BHVO-2 basalt (Experiment 1). The signals were obtained by venting the vapours into an ICP-MS as shown in Figure 1a. The temperature of the hot plate carrying the beaker is indicated. The disappearance of the NO_x signals and the simultaneous sublimation of P and B indicate that the residue dried up at time = 6420 ± 20 s (see text for more details). Time-resolved signals for other elements are reported in Appendices S2 and S3.

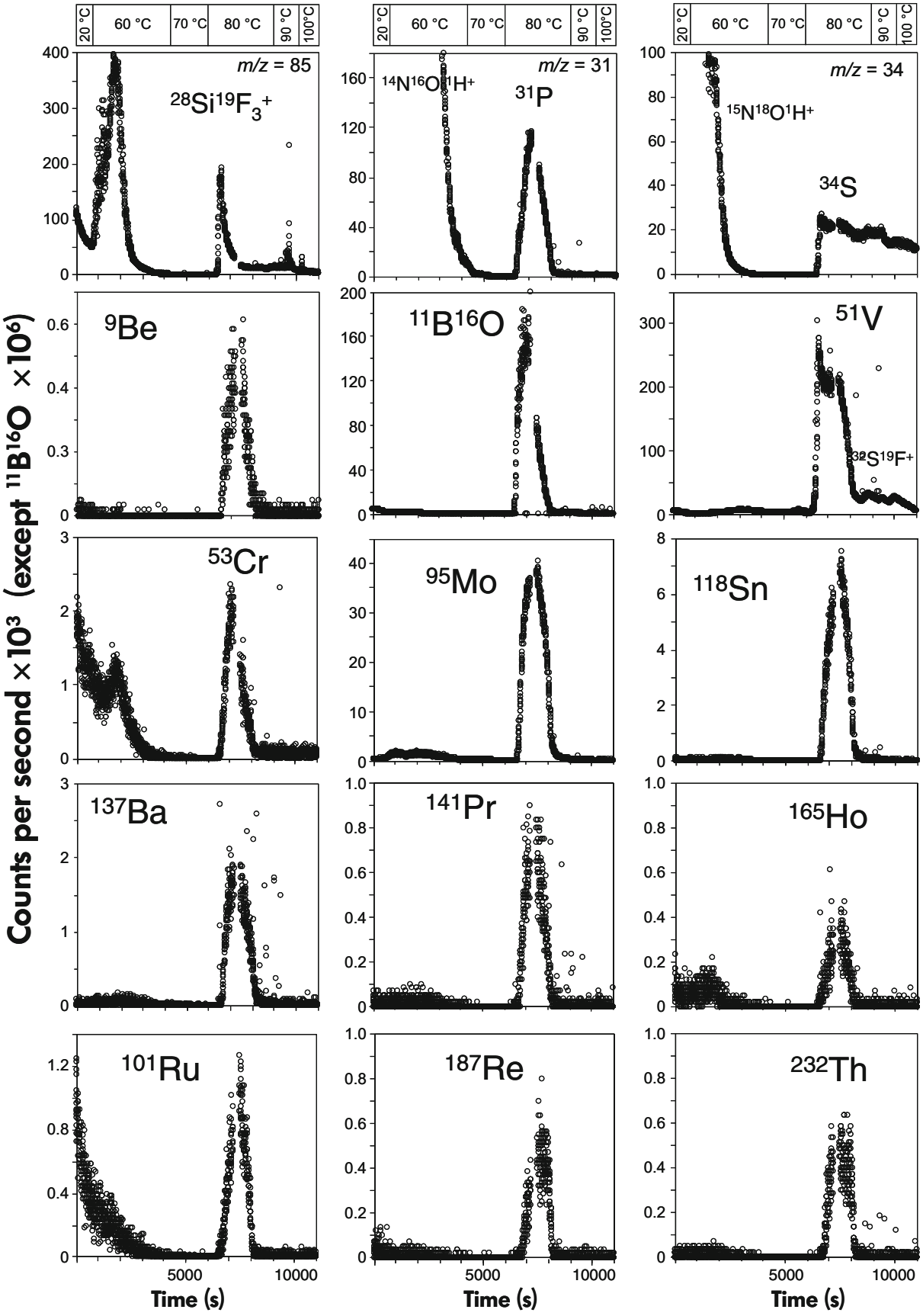

silicon hydroxides and oxides overlap ^{45}Sc ($^{28}Si^{16}O^{1}H^{+}$; $^{29}Si^{16}O^{+}$) and to a lesser extent ^{47}Ti ($^{30}Si^{16}O^{1}H^{+}$). Evaporation of HNO_3 resulted in a decreasing signal of NO_x on which were superimposed P and S signals at m/z of 31 and 34. After drying, the peaks at m/z of 31 ($^{31}P^{+}$) and 69 ($^{31}P^{19}F_2^{+}$) indicate a transient sublimation of phosphorus, whereas sulfur species $^{34}S^{+}$ and $^{32}S^{19}F^{+}$ record a more progressive decreasing sublimation of sulfur.

No less than thirty out of the fifty-seven elements monitored showed a sublimation peak (Table 4a in Appendix S1, Figure 2, Appendices S2 and S3). The peaks lasted about 30 min and were particularly well marked for B, V, Cr, Mo, Ru, Sn and Re, but also occurred surprisingly for a range of refractory elements including Be, some rare earth elements (Ce, Pr, Dy, Ho), Nb, Ba and Th. The sublimation peaks of refractory elements cannot be explained by the interferences of major volatile fluorides. For instance, the signals on ^{51}V and ^{53}Cr cannot be ascribed to $^{32}S^{19}F$ and $^{34}S^{19}F$, respectively, because the relative abundance of $^{51}V/^{53}Cr$ (> 100) is much higher than the $^{32}S/^{34}S$ natural ratio of 22.1. In addition, sulfur monitored at $m/z = 34$ did not show a sublimation peak but a slowly decreasing signal over time. Only the ^{51}V peak tail can be ascribed to $^{32}S^{19}F$ (Figure 2). From the ^{51}V peak/tail ratio (> 8), the contribution of $^{32}S^{19}F$ on ^{51}V is estimated to be less than 15%. The twenty times smaller $^{34}S^{19}F$ signal has a negligible contribution on ^{53}Cr. There was also no interference of Sn fluorides on ^{137}Ba ($^{118}Sn^{19}F$) or ^{141}Pr ($^{122}Sn^{19}F$) because the most abundant Sn species $^{120}Sn^{19}F$ is not detected on ^{139}La. A contribution of Sb oxides can also be ruled out as Sb did not show a sublimation peak. Likewise, no obvious interference accounts for the ^{232}Th peak.

Bulk vapour composition (BHVO-2 experiment 2a)

The composition of the recovered vapour is reported in Appendix S1 (Table 4b), and selected elements are plotted in Figure 3 against the evaporation temperature for experiments stopped before (left) and after drying (right). Element contents are reported as mass fractions (in % *m/m* or μg g^{-1}) relative to the initial amounts of an element in the dissolved BHVO-2 powder from Jochum *et al.* (2016). For each value below the ICP-MS detection limit or three times the procedural blank, we report an upper bound of the mass fraction volatilised. Scandium and palladium are not reported because of major interferences of silicon hydroxides and oxides on ^{45}Sc, and the probable interference of $^{29}Si^{19}F_4^{+}$ on ^{105}Pd. The volatilisation loss of elements generally negatively correlates with the boiling/sublimation temperature of their related fluoride compounds: divalent transition metals (Mn, Co, Ni, Zn, Cu), alkali earth metals, Li, rare earth elements, Y, Ga, U, Th and high field-strength elements (Zr, Hf, Nb, Ta, Ti) volatilise to the smallest extent (mass in vapour condensate/mass in the dissolved BHVO-2 powder < 180 μg g^{-1}). Volatilisation of Rb, Mo, Pt, Pb, Sn, Tl, Bi is more significant (up to 1%), whereas Se, Au, Re, V, Ru and metalloids (B, Ge, As, Sb, Te) volatilise to the largest extent (between 1 and 75%). Duplicate experiments performed at 50 °C and 100 °C are generally consistent with the general volatility sequence, although the extent of volatilisation of individual elements can vary significantly (Table 4b in Appendix S1). The weak reproducibility observed for some elements (e.g., B, As, Te, Sb, Bi) might be related to poorly constrained parameters such as the shape of the fluoride residue or the exact final volume of condensates (drop size) at the end of the concentration step. Beyond this variability, the following robust trends emerged: element evaporation before drying was generally small and barely increasesd with increasing temperature (Figure 3). For most elements, volatilisation occurred mainly after drying through sublimation. Sublimation generally markedly increased with increasing temperature for Se, volatile metals and metalloids (B, Ge, Se, Te, Sb, V, Mo, Ru, Re, Au) and some refractory elements (Ti and Nb). Conversely, sublimation peaked at 50 °C for Hf, Zr, Yb, U, Cu, Zn, Rb, Ba and Sr. Arsenic displayed anomalous behaviour with lower contents at 50 °C vapours collected after drying compared with vapours collected before drying at the same temperature. For vanadium, closed-system sublimation above 80 °C was

Figure 3. Bulk composition of the vapours recovered during closed-system evaporation of HF-dissolved BHVO-2 (Experiment 2). The experiments used the EV-6.25 ml evapoclean device from Analab (Hoenheim, France). Element contents are reported as mass fractions relative to the initial amounts of element in the dissolved BHVO-2 powder: mass fraction volatilised = $(C_{cond} \times m_{cond})/(C_{BHVO\text{-}2} \times m_{BHVO\text{-}2})$, where C_{cond} and $C_{BHVO\text{-}2}$ are the measured concentration of the element of interest in the condensate and its mass fraction in the BHVO-2 powder (Jochum *et al.* 2016), respectively. m_{cond} and m_{BHVO} are the mass of the condensate and that of the BHVO-2 powder digested, respectively. The uncertainty on the fraction volatilised mainly depends on the uncertainty on C_{cond} (given in text). (a) Non-metal and metalloids (in %); (b) volatile transition metals (in %); (c) refractory metals (in μg g^{-1}). Compositions are shown for evaporation stopped before (left) and after drying (right), and temperature ranging between 50 and 100 °C. Data are from Table 4b in Appendix S1.

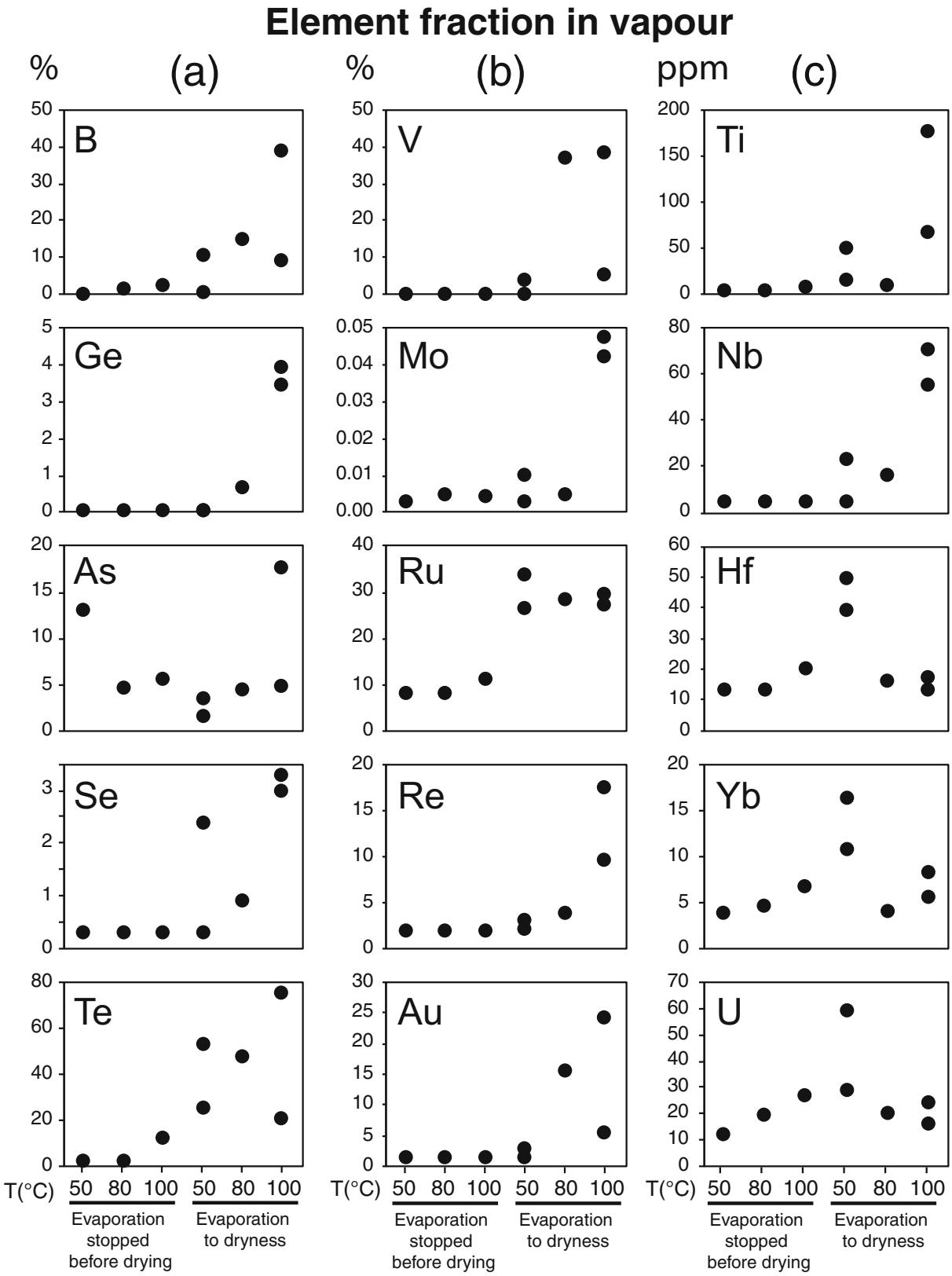

sufficiently important to yield measurable V depletion (up to 32%) in the residues (Table 4c in Appendix S1). For most other elements, the variations of composition of the solid residues were generally within the repeatability of the ICP-MS measurements. The vapours collected after re-dissolution of the dry fluoride residues in 14 mol l^{-1} HNO_3 and evaporation did not contain significant amounts of elements, thereby confirming the role of fluorides in the vapour transport of trace elements.

Results for other rock compositions (experiment 2b)

The results obtained by repeating experiment 2 (evaporation to dryness in the closed system) at 100 °C with BIR-1, AGV-1 and UB-N reference materials are reported in Appendix S1 (Table 4d). Data are plotted in Figure 4 for selected elements together with the mean of the two experiments performed on BHVO-2 under the same conditions (Appendix S1, Table 4b). For elements that are above the limit of detection in a least three reference materials, we derived the following average volatility sequence: Te > Au > Se > Ru > B > V > Re > As > Ge > Pt > Cd > Ag > Sb > Mo > Ti > Nb > Sn > Yb. However, element volatilisation largely varied among the four reference materials: by a factor of 2–4 for Te, Re and B, between 7 and 14 for Ag, Sn, Yb, V, Au, Ti, Mo and Pt, and above 20 for Nb, Ru, Ge, Cd, Se, As and Sb. The BHVO-2 basalt showed the highest volatilisation of B, V, As, Sb and Sn and the lowest loss of Cd, Ag, Ti and Yb. The UB-N serpentinite showed the highest volatilisation of Ti and the lowest loss of Au, Se, Ru, V, As and Ge. The AGV-1 andesite displayed the largest Se and Pt losses and lowest Sb loss, whereas BIR-1 basalt displayed the largest Mo and Nb losses. For several elements (Te, Se, Ru, Pt, Ti, Nb, Mo) the volatilisation loss tended to increase with the decreasing mass fraction of the elements in the silicate rock. This trend could reflect an underestimated blank contribution, underestimated mass fractions of elements occurring in a very low amount in the reference materials, in particular for those elements that are less well characterised (e.g., Se in AGV-1), or preferential volatilisation of minor fluorides phases. We also note that in addition to the largest Mo and Nb losses, BIR-1 showed anomalously high volatilisation of Rb (4.7%), U-Th (0.8–0.9%), Zr-Hf (0.1–0.3%), Gd (387 μg g^{-1}) and heavy rare earth elements (30–100 μg g^{-1}). These anomalies, which are well outside the detection limit, have an unknown origin.

Closed-system *versus* open-system sublimation (BHVO-2)

We combined data from experiments 1 and 2 to evaluate and compare element sublimation under open-system and closed-system conditions at 80 °C for BHVO-2 (Figure 5). We assume that the differences in the experimental setting (test portion size and HNO_3 concentration) between experiments 1 and 2 produced minor biases compared with the differences in element volatilisation that result from evaporating samples in open- and closed-system conditions. The amount of element sublimated during open-system evaporation was estimated from signal integration over the sublimation peaks, as explained in the caption to Figure 5: this amount, reported in Table 4a, exceeds 0.1% only for B (37%), Ru (2.7%), Se (0.3%) and Te (0.15%). It is only 0.08% for Re, 0.02% for Ge and less than 50 μg g^{-1} for other elements. Element sublimation in closed-system conditions was estimated by subtracting the amount of element in vapour collected before drying from the amount of element in vapour collected after drying (Table 4b). As shown in Figure 5, sublimation markedly increased in the closed-system condition for several elements including V (37% *vs.* 1 μg g^{-1}), Ge (0.7 *vs.* 0.02%), Ru (28 *vs.* 2.7%), Sn (0.7% *vs.* 9 μg g^{-1}), Te (47% *vs.* 0.15%) and Re (3.7% *vs.* 0.08%). Moreover, some elements that did not sublimate measurably during open-system evaporation sublimated significantly in closed-system conditions: Au (15%), Bi (0.2%) and Pt-Sb (> 0.04%) (Figure 5). Closed-system conditions also increased the sublimation of some refractory elements (Nb, Ba, Ce, Pr) at or above the μg g^{-1} level (Figure 5). On the other hand, B, Ti and Cr sublimated in similar proportion in the two experiments, while As did not sublimate in the closed system at 80 °C.

Discussion

Closed system *versus* open-system evaporation

Closed-system evaporation has many advantages, reducing sample contamination and avoiding acid gas emissions but strongly modifies the behaviour of elements and yields unexpected effects. The first effect is to markedly increase the sublimation of several elements, in particular V, Ge, Te, Se, Re, Ru, Sn, Au, Bi, Pt and Sb (Figure 5). This effect is contrary to the theory of Langmuir (1916), according to which the rate of sublimation is lower in closed systems due to a higher rate of condensation (back-reaction). To explain this, one should consider that during open-system evaporation the conditions above the evaporating sample are more or less buffered by ambient air, depending on the evaporation rate. In contrast, during closed-system evaporation, the conditions above the evaporating sample are entirely controlled by the evaporating liquid, leading to higher vapour pressures of HF, HNO_3 and H_2O in equilibrium with the liquid and the solid residue after drying. For those elements with multiple valence states, our results suggest that the higher vapour pressure of HF favours the formation of

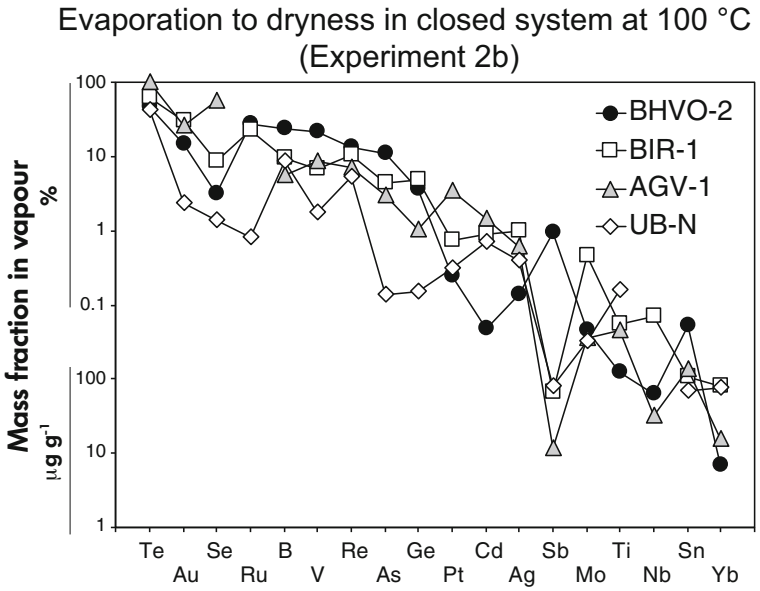

Figure 4. Comparison of bulk vapour composition for four silicate reference materials (BHVO-2, BIR-1, AGV-1 and UB-N). The HF-dissolved silicates were evaporated to dryness at 100 °C in a closed system (Figure 1b). Mass fractions in the vapour condensates are relative to the initial amounts of elements in the dissolved powders (300 mg) calculated using the mass fractions from Jochum *et al.* (2016). The mean of two experiments is reported for BHVO-2. Elements are sorted along the horizontal axis according to the average volatility sequence. Data are from Table 4b and 4d in Appendix S1.

highly fluorinated species with lower boiling or sublimation temperature, such as (Table 1):

VF_3 (1395 °C m.p.) → VF_5 (48 °C b.p.)

GeF_2 (130 °C b.p.) → GeF_4 (-37 °C s.p.)

SeF_4 (102 °C b.p.) → SeF_6 (-47 °C s.p.)

TeF_4 (195 °C b.p.) → TeF_6 (-39 °C s.p.)

ReF_4 (300 °C s.p.) → ReF_6 (34 °C b.p.)

PtF_4 (600 °C m.p.) → PtF_6 (69 °C b.p.)

Molybdenum, U and Cr that potentially form volatile fluorides (MoF_6, UF_6 and CrF_5 with b.p. < 120 °C) do not sublimate importantly (< 500 µg g^{-1}) in closed as in open systems, probably because the most fluorinated compounds are not stable in the conditions of the experiments, and/or the elements co-precipitate with major fluorides. The marked increase in Mo sublimation between 80 and 100 °C (Figure 3) raises the possibility of more extensive sublimation of Mo above 100 °C. Conversely, Sb, Sn, Au and Bi that form fluorides with boiling/sublimation temperatures in the range 141–705 °C (Table 1) sublimate significantly (> 0.1%) in a closed system (Figure 5). A possible explanation is that the higher vapour pressure of H_2O in closed systems enhances the sublimation of these moderately volatile fluorides through the formation of hydrated complexes $(M^{n+}F_n)\cdot nH_2O$. For instance, the role of hydration on metal volatility has been shown for chlorides in hydrothermal systems (Williams-Jones and Heinrich 2005). The sublimation of highly refractory fluorides of rare earth elements (with boiling temperatures in excess of 2000 °C for the dominant trivalent species) requires the contribution of additional processes, such as the formation and decomposition of unstable tetravalent species. While dominant cerium trifluoride is not volatile (boiling point of 2180 °C), less stable cerium tetrafluoride sublimates significantly. The reason is that sublimation of cerium tetrafluoride competes with thermal decomposition to CeF_3 in the solid phase (Chilingarov *et al.* 2015):

$$CeF_{4\ (s)} < {}^{CeF_{4\ (G)}}_{CeF_{3\ (s)}+0.5F_{2\ (G)}} \quad (1)$$

It is possible that similar decomposition/sublimation reactions apply to other rare earth elements (Pr, Dy, Ho) detected in the sublimation vapours (Figure 2 and Appendix S3), especially as rare earth tetrafluorides other than Ce are very unstable and decompose at low temperature (Chilingarov *et al.* 2015). In addition, Yokoyama *et al.* (1999) noted that

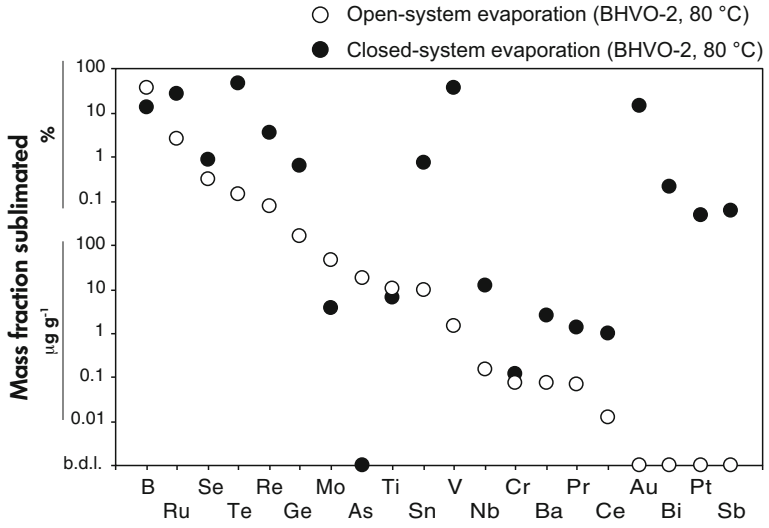

Figure 5. Sublimation of elements at 80 °C during open-system and closed-system evaporation of HF-dissolved BHVO-2. Mass fractions are relative to the initial amounts of element in the dissolved BHVO-2 powder ($C_{BHVO\text{-}2} \times m_{BHVO\text{-}2}$). Open-system data were obtained by integrating the signals over the sublimation peaks measured in experiment 1 (Table 4a in Appendix S1): Mass of element (X) sublimated $= \sum_{C=1}^{C=N} \frac{CPS_{(X)}}{CPng_{(X)}} \times \Delta t_C$ where N is the number of measurement cycle (C) during the sublimation peak (N is ~ 400 and slightly varies depending on element), CPS is the measured signal (in counts per second), CPng is the ICP-MS response (in counts per ng) and Δt_C is the scanning period (4.47 s). Given the high number of measurement cycles during the sublimation peak, the uncertainty on the mass of element sublimated is mostly dependent on the uncertainty of ICP-MS response, which was evaluated to be less than 10% for most elements (and 15–50% for Ge, Te, Ti, Zr and Sr) based on repeated analysis in dry plasma mode of a 500 ng l^{-1} multielement solution (prepared by dilution of a 10 mg l^{-1} certified standard solution). Closed-system data were obtained by subtracting the amount of element in vapours collected before drying to the amount of element in vapours collected after drying (Table 4b in Appendix S1). Elements are sorted from left to right according to the decreasing sublimation of elements during open-system evaporation.

elements with avalence state > 3 do not co-precipitate with major element fluorides, such as $Na_xMg_xAl_{2-x}(F,OH)_6.H_2O$ and $CaMg_2Al_2F_{12}$ and $CaAlF_5$ but form pure fluoride compounds $M^{n+}F_n$. This may contribute to the formation of free REE tetrafluoride prone to sublimation.

Role of temperature

Temperature has a complex influence on element volatilisation. This is especially apparent when evaporation is prolonged to dryness in a closed system (Figure 3). Three types of behaviour can be distinguished: (a) Some elements (V, Ge, B, Te, Sb, Mo, Au, Se, Re) sublimate to a larger degree with increasing temperature. The effect is extreme for V, Ge and Se (10^2–10^3 larger sublimation extent), suggesting the $VF_3 \rightarrow VF_5$, $GeF_2 \rightarrow GeF_4$ and $SeF_4 \rightarrow SeF_6$ transitions discussed in the previous section occur over the 50–100 °C temperature range investigated here. (b) On the other hand, the amount of element in the vapour peaks at 50 °C after drying for elements that generally form less volatile fluorides (Table 1), including Hf, Zr, Yb, U, Cu, Zn, Rb, Ba and Sr. This effect is confirmed by repeating the experiments at 50 and 100 °C (Figure 3c). This unexpected behaviour might be related to specific speciation of elements at low temperature, consistent with the pink colour of the 50 °C residue, when residues formed at higher temperature are greenish (Figure 6). Analysis of the residues by *energy dispersive spectrometry* (EDS) indicates that the colour change results from hydrated ferric fluorides (light pink) being replaced with anhydrous ferric fluorides (green) above 50 °C (Figure 6). This observation, together with the general increase in the F/O ratio with increasing temperature, points to the precipitation of anhydrous fluorides above 50 °C. We hypothesise that the low-temperature precipitation of hydrated complexes $(M^{n+}F_n)\cdot nH_2O$, which are potentially more volatile than the corresponding anhydrous species, could explain the volatilisation of elements forming poorly volatile fluorides. (c) Arsenic displays a third type of behaviour, being the least abundant in vapours collected at 50 °C after drying (Figure 3). This behaviour is anomalous because it requires a flux of As in the opposite direction from the condensates to the solid residue after drying at 50 °C. A

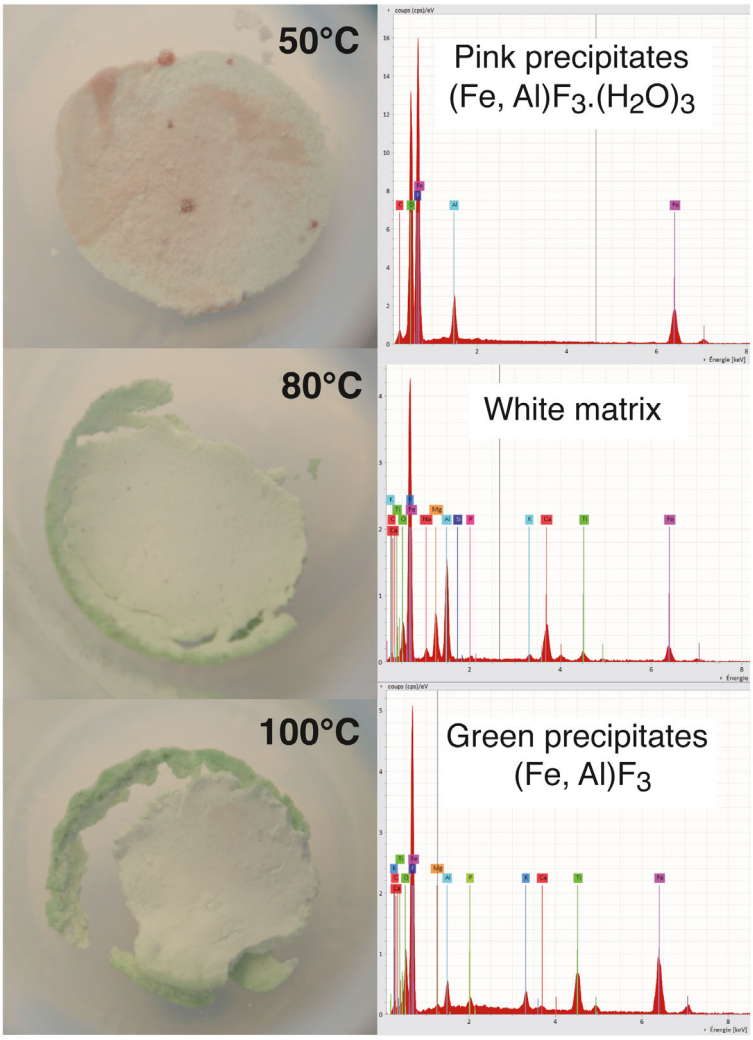

Figure 6. Photographs and EDS spectra of the BHVO-2 fluoride residues after evaporation to dryness in the closed system. Evaporations were conducted at temperatures of 50, 80 and 100 °C. The composition of the residues was investigated by scanning electron microscopy, using a SxFive Tactis Electron Microprobe (Cameca, Gennevilliers, France). Energy dispersive spectrometry spectra are shown for the pink precipitates formed at 50 °C (hydrated Fe-Al fluorides), the white matrix formed at 80 °C and also occurring at lower and higher temperatures (mixture of Ca-Mg-Fe-Al fluorides) and the green precipitates formed at 100 °C (anhydrous Fe-Al fluorides, dominantly).

possible explanation is to consider a first unidirectional transfer of As from the hot acid towards the condensate governed by the partitioning of As between vapour and liquid. After total evaporation, the vapour is in equilibrium with the condensate on one side and with the residual solid phase on the other side of the PTFE elbow. We hypothesise that the new equilibrium between vapour and solid could allow for the adsorption of As gaseous species into the solid (i.e., species with a lower partition coefficient between vapour and solid than between vapour and liquid). Such process could deplete the vapour in As and thus drive an element flux in the opposite direction from the condensate to the solid residue *via* the intermediate vapour phase.

Volatilisation of refractory elements

One of the major and unexpected findings of this study is the detection in the vapour phase of highly refractory elements, such as Th and rare earth elements. Although the extent of volatilisation remains extremely small (at the μg g^{-1} level) and only detectable from the analysis of the vapour (either directly or after condensation), this observation remains puzzling. We discussed above the processes that could potentially allow for the volatilisation of highly refractory elements, such as the decomposition of unstable species and the low-temperature hydration of fluorides. On the other hand, analytical artefacts might also be

considered. Although contamination of the vapour condensates is not negligible, contamination cannot explain the abundance of refractory elements in the condensates, which in many cases are well above the procedural blank and ICP-MS detection limit (Table 4b and 4d in Appendix S1). In addition, sublimation of refractory elements, including Th and rare earth elements, was also detected during the direct analysis of the vapour in experiment 1. Another possible artefact is the mobilisation of solid particulates from the fluoride precipitate due to static electricity. Such a phenomenon is well known especially in PTFE vessels and cannot be totally ruled out here, although macroscopic fluoride particulates were not observed on the walls of the PTFE vessel. Mobilisation of solid particulates from the dry residue is expected to be an erratic process, which could explain the spikes shown by major elements (Mg, Fe, K) on the time-resolved signal acquired during the first experiment (Appendix S2). In this case, the mobilisation of particulates cannot explain the well-defined sublimation peaks shown by trace elements. This decoupling between major and trace elements is consistent with the idea that trace elements incompatible with major element fluorides form free fluorides $M^{n+}F_n$ prone to sublimation. Such a process may be critical for thorium, which quantitatively precipitates as ThF_4 (Yokoyama *et al.* 1999).

Implications

Hydrofluoric acid and inverse *aqua regia* have been alternatively used to dissolve silicates for the determination of PGE and Te, As, Bi, Sb and Se (TABS) (e.g., Rehkämper *et al.* 1998, Wang and Becker 2014, Yierpan *et al.* 2018, Mansur *et al.* 2020). Recent studies (Ishikawa *et al.* 2014, Li *et al.* 2015, Yierpan *et al.* 2018) show that HF-dissolution is generally more effective but potentially causes substantial volatilisation of the elements. However, this work shows that the sublimation of PGE, TABS and other elements forming volatile fluorides, with the exception of B, remains small (< 3%) as long as evaporation is conducted in an open system (Figure 5), making HF dissolution the method of choice for bulk analysis of basalts. Such a conclusion agrees with previous observations of the behaviours of Ge and Se-Te (Luais 2012, Yierpan *et al.* 2018). Conversely, we do not recommend evaporating samples to dryness in a closed system (e.g., a PTFE elbow), which favours the formation and sublimation of fluorides. In such conditions, volatilisation loss can exceed 3% for Te, Au, Se, Ru, B, Re, As, V and Ge. This inference holds for a wide range of silicate compositions according to our experiments on basalt, andesite and serpentinite. Generally, low-temperature (50 °C) evaporation stopped before drying yields minimal loss of elements forming volatile fluorides, with the exception of As which already partitions into vapour at 50 °C (Figure 3). However, a drawback of stopping evaporation before drying is a large amount of remaining Si, whose hydroxides and oxides generate major spectral interferences on the scandium unique isotope (^{45}Sc).

The sublimation of elements forming less volatile fluorides is extremely small and for most elements insignificant compared with the precision of ICP-MS measurements. For closed-system applications potentially relevant to radiochemistry, we do not recommend evaporation to dryness at 50 °C, which favours the formation of hydrated fluorides that are potentially more volatile than anhydrous fluorides formed at a higher temperature. Hafnium, Zr, Yb, U, Cu, Zn, Rb, Ba and Sr seem to be affected by such a process.

Lastly, the extensive sublimation of vanadium in closed systems at 80–100 °C (Figure 3) could be applied to V separation for the purpose of isotope measurement, especially as the major interfering elements Ti and Cr do not sublimate importantly (< 200 μg g^{-1}). Combining closed system (V extraction) and open system evaporation (HF and B elimination) could be an alternative to the five separate ion exchange columns currently used in V isotope studies (Nielsen *et al.* 2011).

Conclusions

Sublimation of trace elements during the evaporation to dryness of an HF-dissolved basalt (BHVO-2) has been investigated under open- and closed-system conditions. The composition of vapours emitted during open-system evaporation was monitored by venting the vapours into an ICP-MS. The time-resolved signal showed a sublimation peak for thirty elements including B, V, Cr, Mo, Ru, Sn, Re and, surprisingly, some refractory elements (Be, Ce, Pr, Dy, Ho, Nb, Ba and Th). However, with the exception of boron, the amount of element sublimated at 80 °C remains small (≤ 3% for Ru, < 0.3% for Se, Te, Re and Ge and < 50 μg g^{-1} for other elements), making open-system evaporation generally suitable for quantitative analyses. Closed-system evaporation is an attractive and simple way to reduce sample contamination and acid gas emissions to the environment. However, experiments conducted in PTFE elbows between 50 and 100 °C showed that closed-system conditions strongly modify the behaviour of elements and produce unexpected effects. Closed-system evaporation first markedly increases the sublimation of elements forming volatile (V, Ge, Se, Ru, Sn, Te, Re, Au, Pt, Sb) and less volatile fluorides (Nb, Ba and rare earth elements). This increase results from the higher vapour pressure of HF that allows for the formation of highly fluorinated species with lower boiling

or sublimation temperatures, or unstable species such as rare earth element tetrafluorides for which sublimation competes with thermal decomposition. Raising the temperature from 50 to 100 °C has contrasted effects depending on elements. On the one hand, high temperature favours the sublimation of highly fluorinated species such as VF_5, GeF_4 and SeF_6, and generally the loss of volatile fluorides of B, Se, Te, Mo, Ru, Re, Au, Ti and Nb. On the other hand, some refractory elements (e.g., Hf, Zr, Yb, U and Cu) preferentially sublimate at 50 °C possibly through the formation of hydrated fluorides. These findings indicate that closed-system evaporation must be used with caution but also suggest that the specific volatility of some elements (e.g., V) could find an application in separation procedures. Repeated experiments on BIR-1 basalt, AGV-1 andesite and UB-N serpentinite indicate that our conclusions are valid for a wide range of silicate composition and point to the following average volatility sequence during evaporation of HF-dissolved silicates: Te > Au > Se > Ru > B > V > Re > As > Ge > Pt > Cd > Ag > Sb > Mo > Ti > Nb > Sn > Yb.

Acknowledgements

We thank two anonymous reviewers for their constructive comments and Jacinta Enzweiler for handling the manuscript and for suggestions. We are grateful to K. Suchorski and J.L. Devidal for photographs and EDS spectra of the fluoride residues, A. Gannoun for sharing reference materials and C. Bosq for help in the clean laboratory. This research was financed by the French Government Laboratory of Excellence initiative no ANR-10-LABX-0006, the Region Auvergne and the European Regional Development Fund. This is Laboratory of Excellence ClerVolc contribution number 534.

Data availability statement

The data that support the findings of this study are provided in the data tables

References

Babel M. and Schreiber B.C. (2014)
Geochemistry of evaporites and evolution of seawater. In: Holland H.D. and Turekian K.K. (eds), Treatise on Geochemistry (2nd edition), 9, Elsevier (Amsterdam, Netherlands), 483–560.

Bajo S. (1978)
Volatilization of arsenic(III, V), antimony(III, V), and selenium (IV, VI) from mixtures of hydrogen fluoride and perchloric acid solution: Application to silicate analysis. Analytical Chemistry, 50, 649–651.

Bock R. (1979)
A handbook of decomposition methods in analytical chemistry. Wiley (New York), 444pp.

Chao T.T. and Sanzolone R.F. (1992)
Decomposition techniques. Journal of Geochemical Exploration, 44, 65–106.

Chilingarov N.S., Knotko A.V., Shlyapnikov I.M., Mazej Z., Kristl M. and Sidorov L.N. (2015)
Cerium tetrafluoride: Sublimation, thermolysis, and atomic fluorine migration. The Journal of Physical Chemistry, 119, 8452–8460.

Hu Z. and Qi L. (2014)
Sample digestion methods. In: Holland H.D. and Turekian K.K. (eds), Treatise on geochemistry (2nd edition), 15, Elsevier (Amsterdam, Netherlands), 87–109.

Ishikawa T. and Nakamura E. (1990)
Suppression of boron volatilization from a hydrofluoric acid solution using a boron-mannitol complex. Analytical Chemistry, 62, 2612–2616.

Ishikawa A., Senda R., Suzuki K., Dale C.W. and Meisel T. (2014)
Re-evaluating digestion methods for highly siderophile element and ^{187}Os isotope analysis: Evidence from geological reference materials. Chemical Geology, 384, 27–46.

Jochum K.P., Weis U., Schwager B., Stoll B., Wilson S.A., Haug G.H., Andreae M.O. and Enzweiler J. (2016)
Reference values following ISO guidelines for frequently requested rock reference materials. Geostandards and Geoanalytical Research, 40, 333–350.

Langmuir I. (1916)
The constitution and fundamental properties of solids and liquids. Journal of the American Chemical Society, 38, 2221–2295.

Li J., Zhao P.P., Liu J.G., Wang X.C., Yang A.Y., Wang G.Q. and Xu J.F. (2015)
Reassessment of hydrofluoric acid desilicification in the Carius tube digestion technique for Re-Os isotopic determination in geological samples. Geostandards and Geoanalytical Research, 39, 17–30.

Luais B. (2012)
Germanium chemistry and MC-ICP-MS isotopic measurements of Fe-Ni, Zn alloys and silicate matrices: Insights into deep earth processes. Chemical Geology, 334, 295–311.

Makishima A. (2016)
Thermal ionization mass spectrometry (TIMS): Silicate digestion, separation, and measurement (first edition). Wiley-VCH Verlag (Weinheim, Germany), 376pp.

Mansur E.T., Barnes S.-J., Savard D. and Webb P.C. (2020)
Determination of Te, As, Bi, Sb and Se (TABS) in geological reference materials and Geo*PT* proficiency test materials by hydride generation-atomic fluorescence spectrometry (HG-AFS). Geostandards and Geoanalytical Research, 44, 147–167.

Menard G., Vlastélic I., Ionov D.A., Rose-Koga E.F., Piro J.-L. and Pin C. (2013)
Precise and accurate determination of boron concentration in silicate rocks by direct isotope dilution ICP-MS: Insight into the B budget of the mantle and B behaviour in magmatic systems. Chemical Geology, 354, 139–149.

Molski M.J. and Seppelt K. (2009)
The transition metal hexafluorides. Dalton Transactions, 3379, 3379–3383.

Nielsen S.G., Prytulak J. and Halliday A.N. (2011)
Determination of precise and accurate $^{51}V/^{50}V$ isotope ratios by MC-ICP-MS, part 1: Chemical separation of vanadium and mass spectrometric protocols. Geostandards and Geoanalytical Research, 35, 293–306.

Pérot B., Jallu F., Passard C., Gueton O., Allinei P.-G., Loubet L., Estre N., Simon E., Carasco C., Roure C., Boucher L., Lamotte H., Comte J., Bertaux M., Lyoussi A., Fichet P. and Carrel F. (2018)
The characterization of radioactive waste: A critical review of techniques implemented or under development at CEA, France. The European Journal of Physics, Nuclear Sciences and Technologies, 4, 3.

Rehkämper M., Halliday A.N. and Wentz R.F. (1998)
Low-blank digestion of geological samples for platinum-group element analysis using a modified Carius tube design. Fresenius' Journal of Analytical Chemistry, 361, 217–219.

Rumble J.R. (editor) (2021)
CRC Handbook of chemistry and physics (102nd edition). CRC Press (Boca Raton), 1624pp.

Sulcek Z., Povondra P. and Dolezal J. (1977)
Decomposition procedures in inorganic analysis. Critical Reviews Analytical Chemistry, 6, 255–323.

Williams-Jones A.E. and Heinrich C.A. (2005)
Vapor transport of metals and the formation of magmatic-hydrothermal ore deposits. Economic Geology, 100, 1287–1312.

Yierpan A., König S., Labidi J., Kurzawa T., Babechuk M.G. and Schoenberg R. (2018)
Chemical sample processing for combined selenium isotope and selenium-tellurium elemental investigation of the Earth's igneous reservoirs. Geochemistry Geophysics Geosystems, 19, 516–533.

Yokoyama T., Makishima A. and Nakamura E. (1999)
Evaluation of the coprecipitation of incompatible trace elements with fluoride during silicate rock dissolution by acid digestion. Chemical Geology, 157, 175–187.

Wang Z. and Becker H. (2014)
Abundances of sulfur, selenium, tellurium, rhenium and platinum-group elements in eighteen reference materials by isotope dilution sector-field ICP-MS and negative TIMS. Geostandards and Geoanalytical Research, 38, 189–209.

Supporting information

The following supporting information may be found in the online version of this article:

Appendix S1. Data tables a, b, c and d.

Appendix S2. Examples of time-resolved signals measured during Experiment 1 (^{24}Mg, ^{39}K, ^{47}Ti, ^{55}Mn, ^{56}Fe, ^{59}Co, ^{65}Cu, ^{66}Zn, ^{69}Ga, ^{72}Ge, ^{75}As, ^{77}Se)

Appendix S3. Examples of time-resolved signals measured during Experiment 1 (^{89}Y, ^{90}Zr, ^{93}Nb, ^{103}Rh, ^{111}Cd, ^{125}Te, ^{133}Cs, ^{139}La, ^{140}Ce, ^{163}Dy, ^{208}Pb, ^{238}U).

This material is available from: http://onlinelibrary.wiley.com/doi/10.1111/ggr.12428/abstract (This link will take you to the article abstract).